Chapter III

Materials and Methods

Chapter-III

MATERIALS AND METHODS

This chapter involves the various methodologies or approaches used for performing the experiments for the fulfillment of the objectives. It deals with the preparation of the materials, collection of sample information and description of all instruments which were employed for data collection. The detailed experimental design related to the objectives are also shown in the form of flow charts in this chapter. Moreover, the methods discussed in this chapter varied based on the collection of qualitative data, quantitative data or both.

3.1 Materials

3.1.1 Raw Material

Two locally cultivated paddies viz. "*Kola Chokuwa*" as low amylose rice (LAR) (12.5 ± 0.13 %) and *Aijong* rice as intermediate amylose rice (IAR) (20.2 ± 0.8%) were procured from the cultivars of Nagaon, Assam, India. The ratio of amylose and amylopectin of paddy was taken into consideration for the present study. The moisture content of the LAR and IAR paddy was observed to be 12 and 12.3% respectively after harvesting (in 2016). The paddy was washed to remove the husk and infested grain and only healthy grains were taken for the experiment.

3.1.2 Chemicals

The chemicals used for analysis in this study were all analytical grade. The reagents were purchased mainly from Sigma, Merck and Himedia. HPLC grade chemicals were used for amino acid analysis.

3.1.3 Machineries and Instruments

Many instruments and machinery were used during the study. An exhaustive list of instruments and machinery along with their make and model and the purpose are presented in Table 3.1.

Table 3.1: Machines used in the study with make and model

Instrument	Make and Model	Purpose
BOD incubator	Model: MES-116B Make: Matrix Eco Solutions Pvt. Ltd	To incubate samples at a particular temperature
Lab grain mill	Model: Pulverisette 14 Make: Fritsch, Germany	To grind samples with a different particle size
Rapid Visco-Analyzer	Model: Starch master 2 Make: Newport Scientific, Warriewood, Australia	To measure the cooking properties of the sample Testing temperature range: 0-99.9ºC Viscosity range: 40–12000 cP
Differential Scanning Calorimeter	Model: 214, Polyma Make: NETZSCH, Germany	To measure the thermal properties of the sample Tempearture range: -170- 600ºC Heating/Cooling rate 0.001 K/min to 500 K/min*
UV-Vis Spectrophotometer	Model: CE7400 Make: CECIL INSTRUMENTS LIMITED, UK	To measure the absorbance of the samples Double beam system Wavlength range: 190-1000nm
Scanning Electron Microscope	Model: JSM 6390LV Make: JEOL, JAPAN	To study the morphology of the samples
X-ray Diffractometer	Model; Rigaku, Mini Flex Make; Japan, Tokyo	To study the structure and physical properties of the sample
Raman spectrophotometer	Model: EZRaman-N analyzer Make: Enwave Optronics Inc., USA	To study the structural fingerprint of molecules Laser: 785 nm Working distance:7mm Pixel Resolution: ~1.45 cm^{-1} per Pixel
Fourier transform Infrared spectrophotometer	Model: Nicolet Impact 410 Make: Thermo Scientific, UK	To study the structural fingerprint of molecules
Bomb Calorimeter	Model: SE-1AC/ML Make: MS. Changsha Kaiyuan Instruments Co. Ltd., Changsha, China	To measure the calorific value of the samples
Kjeldhal machine	Model: ELITE-EX Make: Pelican Equipment	To measure the crude protein content of the samples
Fiber machine	Model: FES 06 Make: Pelican Equipment	To measure the crude fiber content in the samples
Humidity chamber	Model: MES-117A Make: Matrix Eco Solutions Pvt. Ltd	To maintain the samples with a particular humidity
Humidified CO_2 incubator	Hamburg, Germany	To incubate samples with CO_2
Microplate spectrophotometer	Model: Spectra Max Plus 384 Make: Molecular Devices, California, USA	To measure the absorbance of living or dead cells.
Rheometer	Model: MCR 72 Make: Anton Par	To study the flow behavior of samples. Maximum temperature range: -40 to 400 Maximum speed: 1500 rpm

3.2 Work plan pertaining to evaluate the malting characteristics and mechanism of paddy at different germination time and temperature

The work plan pertaining to fulfill the objective # 1 is presented in Fig. 3.1

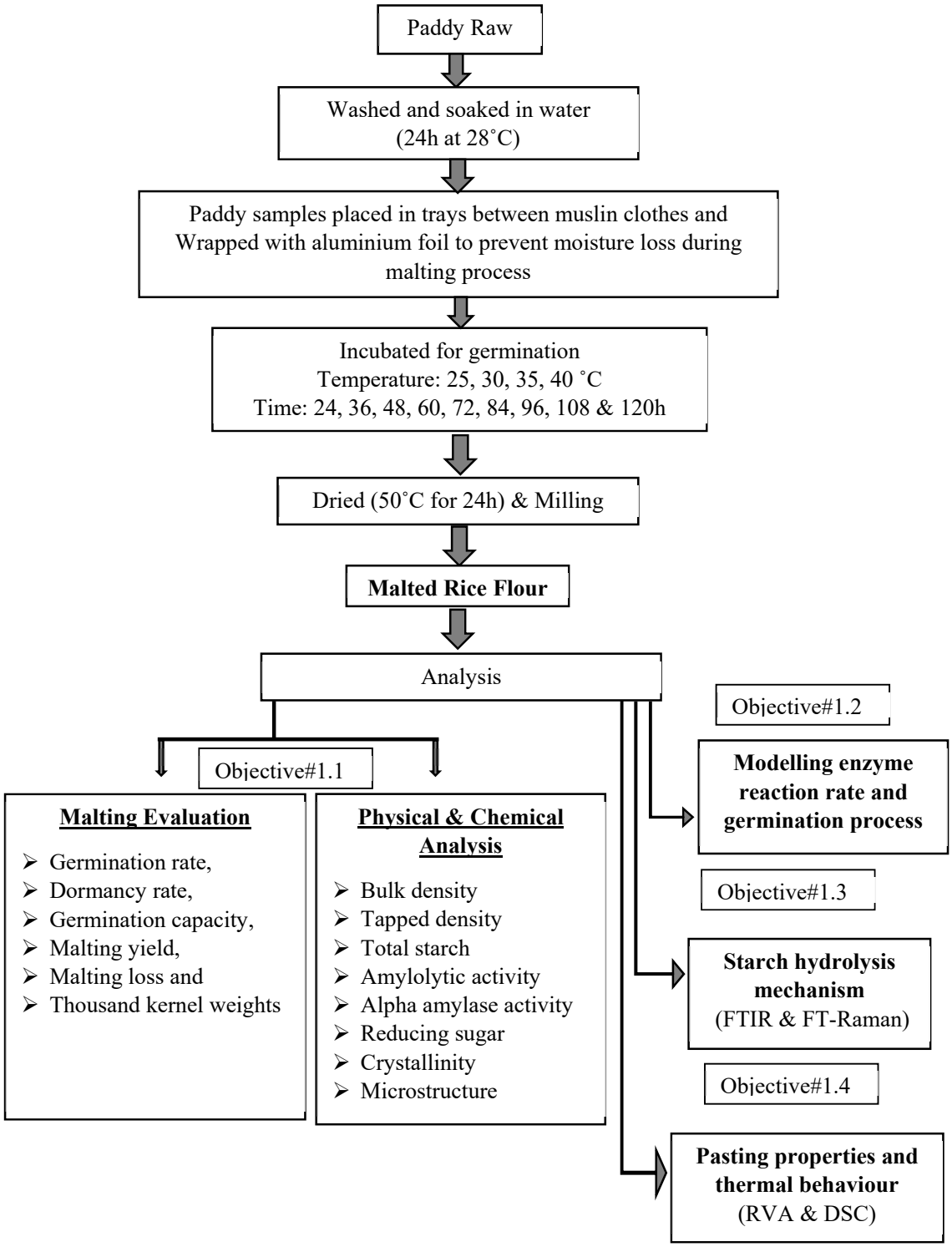

Fig. 3.1 Workplan flowchart of objective # 1

3.2.1 Preparation of raw material and malting of paddy

Malted rice was prepared by three main steps i.e. steeping, kilning and dehusking. Germination of paddy was performed according to the method described by Quadir et al. [30]. Clean and healthy paddy was soaked (stepping) separately in potable water (grain to water ratio 1:3 w/v) at ambient temperature (28°C) for 24h. The water was drained and paddies were once again rinsed once again with 70% ethanol to avoid microbial growth. The paddies were then placed in trays between layers of wet muslin clothes. These trays were wrapped with aluminum foil to avoid moisture loss and thereafter germinated in a temperature-controlled cabinet at four different temperatures i.e. 20, 30 35 and 40°C for 120h. The first sample was drawn after 24h and subsequent samples were drawn at an interval of 12h up to 120h. Each sample was kilned (dried in a hot air oven) at 50°C for 24h. Kilned paddy was dehusked using laboratory de-husker followed by grinding (80µm sieve) using lab grain mill (Pulverisette 14, Fritsch, Germany). It was stored under the refrigerated condition for further analysis. The unmalted rice was taken as the native rice.

3.2.2 Malting potential of germinated paddy

Both paddies were tested for viability by evaluating the malting potential which is described by Germination Rate (GR), Dormancy Rate (DR), and Germination Capacity (GC) [27]. Healthy paddies were soaked in water for 24h at 28°C. The soaked grains (100 Nos each) were placed in wet muslin cloth bag and germinated at four different temperatures (25, 30, 35 and 40°C) separately for 120h. Germination status of each bag was examined after the first 24h and thereafter at an interval of 12h up to 120h by counting germinated and ungerminated grains. Percentage *GR, DR* and *GC* of germinated paddy were calculated using the Eq. 3.1, 3.2 and 3.3 and malting potential was evaluated.

$$GR\ (\%)\ = \frac{Number\ of\ viable\ grains}{Total\ number\ of\ grains} x100 \qquad \text{Eq. (3.1)}$$

$$DR\ (\%)\ = \frac{Number\ of\ unviable\ grains}{Total\ number\ of\ grains} x100 \qquad \text{Eq. (3.2)}$$

$$GC\ (\%) = GR\text{-}DR \qquad \text{Eq. (3.3)}$$

3.2.3 Malting loss and yield of malted brown rice

The germinated paddy at 30 and 35°C was analyzed for its physical properties malting loss and yield of each sample that was calculated by the method given by Ayernor [4]. Rice kernel (100 Nos) were weighed before and after malting. The plumule and radicle (roots) of

malted grains were removed by hand before weighing. The malting loss and yield was expressed as a percentage (g/100g of dry matter) by Eq. (3.4) and Eq. (3.5) respectively.

$$\text{Malting loss (\%)} = \frac{Weight\ of\ unmalted\ grain - Weight\ of\ malted\ grain}{Weight\ of\ unmalted\ grain} x100 \quad \text{Eq. (3.4)}$$

$$\text{Malting yield (\%)} = \frac{Weight\ of\ malted\ grain}{Weight\ of\ unmalted\ grain} x100 \quad \text{Eq. (3.5)}$$

3.2.4 Phyisco-chemical properties of the malted rice flour

3.2.4.1 Physical properties

3.2.4.1.1 Bulk and tapped density

The bulk and tapped density of the malted rice was measured by the method described by Jinapong [18]. The rice flour was transferred into tarred 100ml graduated measuring cylinder up to 100ml and weighed. The measured weight will be used for the determination of bulk density according to the relationship: mass/volume. The tapped density of the sample will be measured by tapping the measuring cylinder 1000 times manually and the volume will be noted for calculation. The results will be measured in duplicates.

3.2.4.1.2 Pasting properties

The pasting properties were determined with a rapid visco-analyser, RVA (Starch master 2, Newport Scientific, Warriewood, Australia) by the method described by Wu et al. [39] with some modifications. The samples (3.2 g, 14 g/100 g moisture basis) were mixed with 25.3 ml of distilled water in canisters. The slurry was mixed at 960 rpm for the first 10 s at 29°C followed by 160 rpm for the rest of the run. The steps for heating and cooling cycles were followed as discussed below:

Step-I: heated to 40ºC for 1 min;

Step-II: heated up to 50ºC within 3 min;

Step-III: heated to 95°C within 3.4 min;

Step-IV: holding at 95ºC for 3 min;

Step-V, and subsequently cooled to 50°C.

The parameters evaluated were the pasting temperature (PT), peak viscosity (PV), hot paste viscosity (HPV), breakdown viscosity BDV), setback viscosity and cold paste viscosity (CPV). The breakdown viscosity (BDV) was calculated as the difference between IPV and HPV, and the setback viscosity (SBV) was equal to the difference between CPV and HPV.

3.2.4.1.3 Thermal behavior

The thermal behavior of samples was measured employing a differential scanning calorimeter (DSC) (214, Polyma, NETZSCH, Germany) by the method described by Park et al. [28]. The samples were saturated with distilled water (1:3) and placed in an aluminum pan and allowed to reach equilibrium overnight. The pan was sealed with a lid for examination under DSC. The reference employed for the measurement was an empty pan with the lid. The samples were heated from 20°C to 150°C at a heating rate of 10 K/min. The onset (TO), peak (TP) and completion (TC) temperatures were computed from the thermogram.

3.2.4.1.4 Kinetics of pasting and thermal properties

Changes in pasting properties and thermal behaviour with respect to germination time were modelled with the zero, first and second order kinetics (Eq 3.6 to 3.8, respectively) [24] and rational function (Eq 3.9), respectively. The rate constants (k_1, k_2 and k_3) for the changes were estimated from the slope of the plots against time arising from Eq 3.6 to 3.8. The rational function employed for the thermal behaviour could be defined as the ratio of two polynomial functions. If P(x) and Q(x) were the polynomials, then a function of the form R(x) =P(x)/Q(x) was a rational function where Q(x) ≠ 0. Eq. (3.9) was a combination of linear and quadratic functions of time t which were represented by the numerator and denominator, respectively.

$$A_t = k_0 t + A_0 \qquad \text{Eq. (3.6)}$$

$$\ln A_t = k_1 t + \ln A_0 \qquad \text{Eq. (3.7)}$$

$$\frac{1}{A_t} = -k_2 t + \frac{1}{A_0} \qquad \text{Eq. (3.8)}$$

Here, A_t and A_0 were the values at the beginning and after the treatment time t. The model with the maximum R^2 was selected to represent the dependency of the input variables.

$$Y = \frac{a+bt}{1+ct+dt^2} \qquad \text{Eq (3.9)}$$

Here, y was equal to T_O, T_P and T_C, and a, b, c, d were the model parameters. The estimation of the parameters of Eq. 3.6 was performed by employing the curve fitting tool of MATLAB, version 2014.

3.2.4.2 Chemical Analysis

3.2.4.2.1 Total Starch, Amylose, amylopectin and reducing sugar content

The starch content of both rice was determined by the method described in AOAC [3]. The total reducing sugar was measured by the dinitrosalicylic acid as described by Saqib [33]. Amylose content was determined in triplicates by the method suggested by Labuschagne et al. [22]. 1 mg of rice flour was soaked with 95% ethanol followed by addition of 9ml of 1M sodium hydroxide to prepare the dispersion and thereafter stirred using a vortex mixer. The samples were placed in a boiling water bath for 15 min and stirred using a vortex mixer every 5 min. The samples were then cooled for 1 h to reach the room temperature and centrifuged at 3000 rpm for 5 min. Thereafter, 0.1 ml of aliquots of the solution were transferred to clean test tubes and 0.1 ml of 1 M acetic acid was added to each test tube followed by the addition of 0.2 ml of iodine solution and 9.6 ml of distilled water. The contents were then mixed in the vortex mixer and incubated for 20 min. The absorbance of the sample was read at 620 nm in a spectrophotometer (CECIL, CE7400) against the reagent blank. The amylose content was calculated from the standard amylose graph. Amylopectin content was calculated by subtracting amylose content from the total starch content as detailed by Wu et al. [39]. All measurements were done in triplicate to avoid experimental error.

3.2.5 Enzyme activity determination

3.2.5.1 Enzyme Extraction

One gram of malted rice was mixed with 10ml of ice-cold 10mM $CaCl_2$ solution and the mixture was incubated at 4°C overnight for enzyme extraction. It was centrifuged at 3000 rpm for 20 min in a refrigerated centrifuge (4°C) and the supernatant obtained was used as enzyme extract for analysis of total amylolytic and α-amylase activity [31].

3.2.5.2 Amylolytic and α-amylase activity

The Amylolytic activity was determined by measuring the amount of reducing sugar produced by hydrolysis of starch using DNSA method [2] with slight modification. Enzyme extract (1ml) and 1% starch solution was mixed in 1:1 ratio and incubated at 27°C for 15 minutes. DNSA reagent (3ml) was added to stop the hydrolysis of starch. The solution was heated in boiling water for 5 minutes and developed colour was measured at 560nm in a UV-Vis spectrophotometer (CECIL, CE7400). Maltose (200µg/ml) was used as a standard for estimation of reducing sugar. The alpha-amylase activity was determined similarly by the DNSA method except that the extracted enzyme was incubated at 70°C for 15min to inactivate β-amylase and debranching enzyme [37]. One unit of enzyme activity (U) was

defined as the amount of micromoles of maltose produced per minute under the test condition and calculated using the formula given by [2].

$$Activities\ (U/ml) = \left(\frac{(mg/ml\ (maltose)\ x\ 10^3}{Molecular\ weight\ of\ maltose\ x\ time\ (\text{min})}\right) x\ 2 \quad \text{Eq. (3.10)}$$

3.2.6 Morphological and structural analysis

3.2.6.1 Scanning Electron Microscopy

The morphological properties of the native rice powder and malted rice were studied from the micrographs captured at 5000X using SEM (JSM-6390 LV, Japan, PN unction type, semiconductor detector) as described by [39] with some modifications. An accelerating potential of 20kV was used for capturing micrographs.

3.2.6.2 Wide angle X-ray scattering

The X-ray diffraction pattern for the native rice powder and malted rice was obtained from the X-ray diffractometer (Rigaku, Mini Flex, Japan, Tokyo) with a K-value of 1.54040 operating at 30kV acceleration potential and 15mA current with a copper target. The diffraction data was calculated over an angular range (2θ) from 10-40° with a scanning speed of 8 deg/min. The percent crystallinity was calculated in Origin pro 8.5 software package by using the formula [26].

$$\%\ \text{Crystallinity} = \frac{Area\ under\ the\ crystalline\ peaks}{Total\ area\ under\ the\ peaks\ (amorphous+crystalline\ peaks)} x100 \quad \text{Eq. (3.11)}$$

3.2.7 Vibrational spectroscopy

3.2.7.1 Raman spectra measurement

FT-Raman spectra was obtained using EZRaman-Analyzer with Narrow Linewidth Diode Laser at 785 nm (or 532 nm) with a maximum power of 350 mW. The system was equipped with two-dimensional CCDs array detector and a fiber optic probe. The probe was attached to a vertical 3-d translational stage with laser light (lens tube) and the sample was placed approximately 7 mm away from the lens tube. Data were collected at 2 cm^{-1} resolution and spectra were obtained in the Raman shift range between 400 and 4000 cm^{-1} [20]. The experiments were conducted in duplicate and spectrum was plotted.

3.2.7.2 FTIR measurement

The analysis was performed by mixing properly dried rice with desiccated KBr in a mortar pestle and pressed into thin pellets by the method given by Kizil [20]. The IR-spectrum of

the sample was obtained using FTIR spectrophotometer (Nicolet Impact 410, Thermo Scientific, UK) equipped with KBr optics and a DTGS detector. Bands at 400–4000 cm^{-1} were scanned with a resolution of 2.0 cm^{-1}. The spectrum was collected in duplicate.

3.3 Modelling enzyme reaction rate and germination process using ANN approach

3.3.1 Theoretical Consideration

Enzymes are mainly accountable for the various biochemical and physiological reactions that occur in all living organisms [5]. The principal for the kinetic study is to find an accurate model equation that has the capability to estimate the reaction rate as similar to the experimental reaction rate. In the kinetic study, all model equations provide error values which have to be minimized. Basically, the error value is low for an enzymatic reaction that follows simple enzyme kinetics. However, it is difficult to find a proper model for in situ reaction enzymatic reaction process that takes place during germination. Germination is a complex process which commences with the uptake of water by the seeds and concludes with the emergence of the embryo. Generally, in enzyme kinetics reaction a particular substrate concentration is maintained and the enzyme is added and thereafter the reaction rate is evaluated with the help of Michaelis-Menten equation. However, in the process of germination, a continuous production of hydrolytic enzymes occurs that is induced by gibberellic acid and breaks down starch resulting in the simultaneous release of reducing sugar. Thereby, with a change in the reaction conditions, the usability of the Michaelis-Menten equation was not appropriate and therefore an alternative method for estimation of the reaction rate was investigated. The Boltzmann function was reported to fit most of the time course data of the biochemical reactions with a high accuracy [5] and therefore this function was employed in this study to determine the enzymatic reaction rate during germination. The obtained reaction rate was further used to model the enzyme kinetics reaction by modified Michaelis-Menten equation and Artificial Neural Network (ANN).

3.3.2 Estimation of reaction rate during germination

Estimation of the reaction rate during the process of germination was performed by employing Boltzmann function. From the time course data, the enzymatic reaction rate was determined in two steps:

(i) Experimental time course data was fitted to the Boltzmann function {Eq. (3.12)}.

$$S = \frac{A_1 - A_2}{1 + exp\left(\frac{t - t_0}{dx}\right)} + A_2 \qquad \text{Eq. (3.12)}$$

Where S = substrate, A_1= constant in Boltzmann function, A_2 = constant in Boltzmann function, dx = with of Boltzmann function, t = reaction time (min), t_0 = constant in Boltzmann function.

(ii) Eq. (3.12) was derived with respect to t and Eq. (3.13) was obtained. This equation could be used to determine Reaction Rate (dS/dt) at any reaction time (t).

$$-\frac{ds}{dt} = \frac{(A_1 - A_2)\left(exp\left(\frac{t-t_0}{dx}\right)\right)}{dx\left(1+exp\left(\frac{t-t_0}{dx}\right)\right)^2} \quad \text{Eq. (3.13)}$$

Where, S = substrate concentration, t_0 = initial time, t = germination time in h, dx = width of Boltzmann function which is taken as the total change in the substrate concentration and dS/dt = reaction rate.

3.3.3 Michaelis-Menten Kinetics

The expression for Michaelis-Menten equation is

$$V = \frac{k_3\, E_t[S]}{k_m + [S]} = \frac{V_m[S]}{k_m + [S]} \quad \text{Eq. (3.14)}$$

Where, V = reaction rate, V_m = maximum reaction rate for the totally saturated enzyme, K_m = substrate concentration when the reaction rate reaches half of the maximum rate

3.3.4 Stochastic Model

According to the enzymatic reaction can be divided into two steps:
We know,

$$E + S \underset{k_2}{\overset{k_1}{\rightleftarrows}} [ES] \xrightarrow{k_3} E + P \quad \text{Eq. (3.15)}$$

$$\frac{dp}{dt} = V = k_3[ES] \quad \text{Eq. (3.16)}$$

$$k_1[E][S] = k_2[ES] + k_3[ES] = [ES](k_2 + k_3)$$

$$[ES] = \frac{k_1[E][S]}{k_2 + k_3} = \frac{[E][S]}{\left(\frac{k_2+k_3}{k_1}\right)} = \frac{[E][S]}{k_m}$$

$$\therefore [ES] = \frac{[E][S]}{k_m} \quad \text{Eq. (3.17)}$$

We know that, $[E] = [E_t] - [ES]$

Where, $[E_t] =$ Enzyme concentration is the function of time

Putting the value of E in Eq. 3.17 we get,

$$[ES] = \frac{([E_t]-[ES])[S]}{k_m} = \frac{[E_t][S]-[ES][S]}{k_m}$$

$$[ES]k_m = [E_t][S] - [ES][S]$$

$$[ES]k_m + [ES][S] = [E_t][S]$$

$$[ES] = \frac{[E_t][S]}{k_m+[S]} \quad \text{Eq. (3.18)}$$

Putting the value of V from Eq. 3.16 to Eq. 3.17 we get,

$$\frac{V}{k_3} = \frac{[E_t][S]}{k_m+[S]}$$

$$V = \frac{k_3[E_t][S]}{k_m+[S]} \quad \text{Eq. (3.19)}$$

If the enzyme concentration varies with the different concentration of substrate w.r.t time, the enzyme will be replaced by a function of time and reaction order. In the same way, for cooperating the behavior, the substrate will also be replaced by a function of time and reaction order. So, the Eq. 3.19 will be modified to Eq. 3.20:

$$V = \frac{k_3|E_t|_m|[S]_t|_n}{(k_m+|[S]_t|_n)} \quad \text{Eq. (3.20)}$$

By denoting the k_3 and k_m value with empirical constants K_1 and K_4 respectively, we get

$$V = \frac{K_1|E_t|_m|[S]_t|_n}{(K_4+|[S]_t|_n)} \quad \text{Eq. (3.21)}$$

This is the final equation after derivation. Here 'm' and 'n' is the order of reaction; E_t and $[S]_t$ is the function of enzyme production and substrate concentration with respect to time (t).

3.3.5 Order of reactions

Based on the order of reaction of substrate and enzyme during the germination of rice, modified non-MM kinetics equation was used. The equations used for zero, first and second order of reactions are shown below:

Zero-order $A = A_0 - kt$ Eq. (3.22)

First order $A = A_0\exp(-kt)$ Eq. (3.23)

Second order $A = \frac{A_0}{(1+A_0kt)}$ Eq. (3.24)

3.3.6 Process modeling of starch germination by using the Artificial Neural Network (ANN)

Artificial Neural Network was applied to model germination process which is also known as the black box model. Essentially, artificial neural networks are designed in an attempt to mimic the methods of information processing and knowledge acquisition of the human brain [5]. Based on the natural neuron, ANN model is developed. In ANN modeling, information processing occurs as a result of interaction through a large number of simulated neurons. Input layer, hidden layer, summation function, threshold function and output layer are the important component of the artificial neural network.

The artificial neural network was developed with the help of different weights which connects various processing elements (Fig. 3.2). Interconnection strengths or weights connect each layer with the proceeding layer. In a Neural network, W_{ih} are the interconnection weights of the input layer (L_I) and hidden layer (L_H), whereas W_{ho} are the interconnection weights of hidden layer (L_H) and the output layer (L_O). Backpropagation is used to adjust the weight in order to minimize the errors. It is done by correction of initial estimated weight values (i.e., W_{ih} and W_{ho}) during training process as obtained in the comparison between predicted outputs and known outputs. Input layer (L_I) and output layer (L_H) are composed of different neurons which consist of input and output of the process, respectively. In this ANN modeling, H_{oj} and O_j are denoted as output for j^{th} neuron of hidden layer and output layer respectively [7,9].

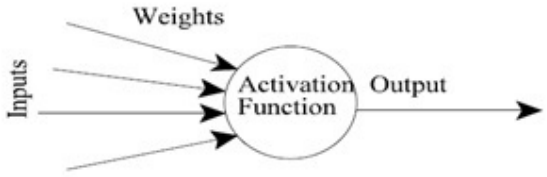

Fig. 3.2 Artificial Neuron

For j^{th} neuron, total input to hidden units is given by H_{ij} which is a linear function of outputs x_i and weights (w_{ij}) on these connections.

$$H_{ij} = \sum_i x_i w_{ij} \qquad \text{Eq. (3.25)}$$

H_{oj} is a real-valued output of the hidden unit. An extra input in the name of bias (θ_j) was also introduced to each unit which had a value of 1. The output of the j^{th}neuron from the hidden to output layer is given by the equation Eq. (3.26).

$$H_{oj} = \frac{1}{1+exp\left(-(H_{ij}+\theta_j)\right)}$$ Eq. (3.26)

The activation function used for neural network calculation was a sigmoid function. The mathematical equation of sigmoid function is shown in Eq. (3.27).

$$f_{act}(x) = \frac{1}{1+exp(x)}$$ Eq. (3.27)

In this study, the experimental data were divided into three parts: training, testing and validation respectively. ANN modeling was done by programming in MATLAB R2014a. A feed-forward neural network was used for the analysis. The network consisted of two neurons in the input layer and four neurons in output layer. Whereas, neurons in the hidden layer was varied with every run until minimum mean square error (MSE) was obtained.

3.4 Weaning formulation based on its physico-chemical and nutritional properties

The formulation of instant weaning food and its physico-chemical and nutritional properties was planned in objective # 2. The detail work plan pertaining to this objective is presented in Fig. 3.3.

3.4.1 Weaning formulation

In developing countries malnutrition among the weaned infants (6 to 12 months) and preschool children (3-5 years) is a major problem due to poverty and illness. Weaning formulations available in the market are beyond the reach of common people as they are very expensive owing to their high processing cost. So, they feed their children with food such as porridges prepared from locally available cereals and tubers. These porridges are rich in starch which increases the dietary bulk since the starch swells and gelatinizes to become thick and voluminous when cooked with water. So, more water is added for easy feeding which eventually lowers the energy and nutrient contents. Therefore, use of malted cereals in weaning formulation can be a solution to this problem which reduces the dietary bulk and increases the calorie intake [32].

3.4.2 Selection of ingredients

The ingredients for formulating the weaning formulation were selected based on the recommended daily allowance as mentioned by [32]. The ingredients selected were whole wheat flour, rice flour, pulse flour, malted rice flour (IAR germinated for 24h at 35°C), whole milk powder and Bhim Kol (*Musa balbisiana*), whole wheat flour (Ashirbad, ITC Ltd), pulse flour (Patanjali), whole milk powder (Patanjali) were purchased from the market

and rice flour was prepared from locally available Aijung rice which was ground into powder in a food processor (Usha 2663).

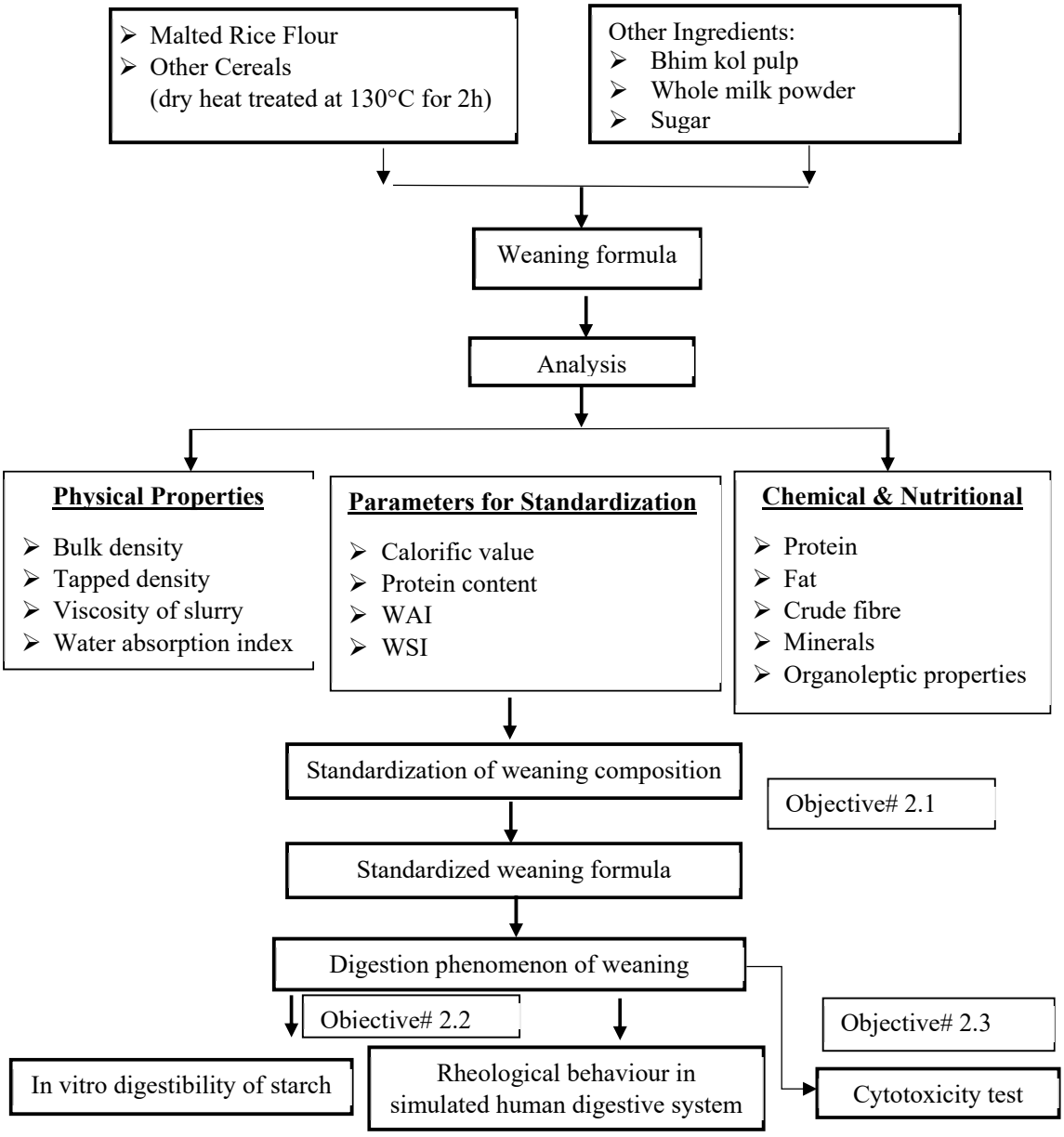

Fig. 3.3 Work plan flowchart of objective # 2

3.4.3 Modification of ingredients by dry heat treatment

The modification of ingredients was employed by the method described by Sun et al. [35]. The ingredients such as whole wheat flour, rice flour, pulse flour and malted rice flour were heated in an electric hot air oven at 130°C for 2h. This process causes physical modification of starch without damaging the granule structure. It also improves the functional properties

of starch and increases the taste and flavour of the ingredients. After dry heat treatment, the flours were packed in containers and stored under refrigeration for further analysis.

3.4.4 Physico-chemical properties of the ingredients

3.4.4.1 Determination of energy content and crude protein content

The gross energy content of the ingredients was estimated by the bomb calorimeter (Make: Ms. Changsha Kaiyuan Instruments Co. Ltd., Changsha, China Model: SE-1AC/ML) method. The crude protein was determined by the Kjeldahl method [3] which was based on the determination of the amount of reduced nitrogen (NH_2 and NH) present in the sample. The ingredients were treated with concentrated sulphuric acid during which various nitrogenous compounds were converted into ammonium sulphate. The ammonium sulphate formed were decomposed by sodium hydroxide and the ammonia produced was absorbed in excess of the neutral boric acid solution and thereafter titrated with a standard acid. The moisture content was measured by the vacuum oven method for 24 h at 70°C.

3.4.4.2. Pasting properties of the modified ingredients

The pasting properties were determined with a rapid visco-analyser, RVA (Starch master 2, Newport Scientific, Warriewood, Australia) and the method was similar as mentioned in section 3.2.4.1.2.

3.4.5 Formulation of weaning food

3.4.5.1 Experimental design

The D-optimal mixture design methodology was used to optimize the levels of ingredients of the weaning formulation. Mixture design is defined as a special type of RSM in which the factors are the components of a mixture and the response varies as the proportions vary. D-optimal mixture design (DMD) which is a type of mixture design, is an effective technique where the total amount of the components is held constant when proportions of the mixture components change [40]. The experimental details and statistical analysis was performed by employing Design-Expert version 7.0.0. Based on literature the portion size of each ingredient required for baby per day (6-12 months) was prepared. The dry heat-treated flours (viz. Whole wheat flour; Rice flour; Pulse flour and Malted rice flour), whole milk powder and fruit were used for weaning formulations and their ranges are presented in Table 3.2. The responses were crude protein content, energy content, water absorption index (WAI) and water solubility index (WSI). A total of 31 combinations were obtained from the mixture design which is shown in Table 3.3. The quadratic model was employed

to the experimental data and the statistical significance was determined by the analysis of variance (ANOVA).

Table 3.2: List of ingredients with their range and responses to experimental design

Ingredients	Code	Moisture (%)	Range	Response
Whole wheat flour	WF	6-7%	10-20%	➢ Protein ➢ Calorific value ➢ Water absorption index ➢ Water solubility index
Rice flour	RF	6-7%	10-20%	
Pulse flour (Bengal gram)	Pulse	6-7%	5-10%	
Whole milk powder	WMP	6-7%	40-50%	
Fruit (*Bhim Kol*)	FR	75-80%	20-25%	
Malted rice flour	MR	6-7%	5-10%	
Vegetable oil (10%) was fixed and added to all the formulations				

Table 3.3 Experimental combinations used in the study

Run	WF (%)	RF (%)	Pulse (%)	WMP (%)	Fruit (%)	MR (%)
1	10.0	15.0	10.0	35.0	20.0	10.0
2	10.0	10.0	5.0	40.0	30.0	5.0
3	10.0	10.0	5.0	50.0	20.0	5.0
4	10.0	10.0	10.0	35.0	30.0	5.0
5	15.0	10.0	5.0	45.0	20.0	5.0
6	15.0	10.0	5.0	35.0	30.0	5.0
7	17.5	17.5	5.0	35.0	20.0	5.0
8	20.0	10.0	5.0	35.0	25.0	5.0
9	10.0	20.0	5.0	35.0	20.0	10.0
10	20.0	10.0	10.0	35.0	20.0	5.0
11	10.0	20.0	10.0	35.0	20.0	5.0
12	10.0	15.0	5.0	45.0	20.0	5.0
13	10.0	10.0	10.0	35.0	25.0	10.0
14	10.0	10.0	5.0	45.0	20.0	10.0
15	10.0	10.0	10.0	45.0	20.0	5.0
16	10.0	10.0	10.0	40.0	20.0	10.0
17	10.0	15.0	5.0	35.0	25.0	10.0
18	15.0	10.0	5.0	45.0	20.0	5.0
19	10.0	15.0	5.0	35.0	30.0	5.0
20	15.2	11.5	7.2	36.3	21.5	8.4
21	10.0	20.0	5.0	40.0	20.0	5.0
22	17.5	17.5	5.0	35.0	20.0	5.0
23	20.0	10.0	7.5	37.5	20.0	5.0
24	15.2	11.5	7.2	36.3	21.5	8.4
25	10.0	15.0	10.0	35.0	25.0	5.0
26	20.0	10.0	5.0	35.0	20.0	10.0
27	10.0	10.0	5.0	35.0	30.0	10.0
28	10.0	20.0	5.0	35.0	25.0	5.0
29	20.0	10.0	5.0	35.0	20.0	10.0
30	20.0	10.0	10.0	35.0	20.0	5.0
31	10.0	10.0	5.0	45.0	25.0	5.0

3.4.5.2 Responses for experimental design

3.4.5.2.1 Energy content, Crude protein content, Water solubility index (WSI) and Water absorption index (WAI)

The energy content and crude protein content were estimated and mentioned in section 3.4.4.1. WAI and WSI were determined in triplicate following the method described by Sawant et al. [34]. 1g sample was suspended in 20 ml of distilled water in a tared 45 ml centrifuge tube and stirred with glass rod. Thereafter, the mixture was kept in water bath for 30 min at 30℃ and then centrifuged at 3,000 rpm for 15 min. The supernatants were poured into dry evaporator dishes of known weight and stored overnight at 120℃ for the process of evaporation. Water solubility index (WSI) and water absorption index (WAI) were expressed as follows:

$$WAI\ (g/g) = \frac{Weight\ of\ dry\ solids\ in\ supernatant}{Dry\ weight\ of\ sample} \quad \text{Eq. 3.28}$$

$$WSI\ (\%) = \frac{Weight\ of\ dissolved\ solids\ in\ supernatent}{Weight\ of\ dry\ samples\ in\ the\ original\ sample}\ x\ 100 \quad \text{Eq. 3.29}$$

3.4.5.3 Standardization and Validation of the weaning formulation

The developed weaning formula was optimized based on the energy content, water absorption index (WAI) and water solubility index (WSI). The optimized results found using 'Design-Expert software was verified by measuring its energy and protein content, WAI and WSI as per methods are given in section 3.4.5.2.1. The percentage error was calculated as the difference between the experimental value and predicted value divided by the experimental value.

3.5 Estimation of solid water ratio of weaning formula and its effect on viscosity

The determination of solid water ratio in weaning formulation is essential to improve the energy intake in young children. In this study the viscosity of the weaning formula was estimated by taking into consideration three levels of solid water ratio was taken (50:50, 55:45 and 60:40) at three different temperatures (35, 40 and 50°C). The viscosity obtained was analyzed to find the optimum ratio for the feeding of the infants. Apparent viscosity was measured in RVA (New Port Scientific, RVA starch master 2, Australia) according to Kapoor [19]. Weaning formulation (3.2g) was dispersed in 25.3ml of distilled water in the canister and mixed using paddle blade. The paddle was allowed to rotate at 160 rpm for 60 seconds and viscosity was recorded at the above-mentioned temperature.

3.6 Physico-chemical and cytotoxicity of the optimized weaning formula

The moisture content analysis was performed by the vacuum oven method at 70°C for 24 h. The ash, fat and crude protein were analyzed by the standard AOAC [3] method.

3.6.1 Hydration property of weaning formulation

The water holding capacity (WHC) and water binding capacity (WBC) was determined by the method described by Cornejo [10]. The WHC can be defined as the amount of water maintained by the sample without being the application of any stress. It was analyzed by adding 1.00g ±0.001 g of weaning formulation in 10 ml of distilled water and was kept at room temperature for 24h. WHC was expressed as grams of water retained per gram of solid. WBC can be defined as the amount of water retained by the sample under low-speed centrifugation. It was determined by mixing 1.000 g±0.001 g of developed weaning formula with distilled water (10 ml) and centrifuged at 2000×g for 10 min. WBC was expressed as grams of water retained per gram of solid.

3.6.2 Bulk and tapped density

The bulk and tapped density of the weaning formula was measured by the method described by in section 3.2.4.1.1.

3.6.3 Flowability and cohesiveness of weaning formula

Flowability and cohesiveness of the weaning formula were evaluated in terms of Carr index (CI) and Hausner ratio (HR), respectively as described by [18]. Both CI and HR were calculated from the bulk (ρ_{bulk}) and tapped (ρ_{tapped}) densities of the powder as shown below:

$$CI = \frac{(\rho_{tapped} - \rho_{bulk})}{\rho_{tapped}} \times 100 \quad \text{Eq. (3.30)}$$

$$HR = \frac{\rho_{tapped}}{\rho_{bulk}} \quad \text{Eq. (3.31)}$$

3.6.4 Particle density and porosity of weaning formulation

The particle density was measured using gas pycnometer (PYC-100A, Porous Materials, Inc). The porosity (Ɛ) of the weaning formula was estimated by using the relationship between the tapped (ρ_{tapped}) and particle ($\rho_{particle}$) densities of the powder as described by Jinapong [18].

$$Porosity\ (\text{Ɛ}) = \frac{(\rho_{particle} - \rho_{tapped})}{\rho_{particle}}\ X\ 100 \quad \text{(Eq. 3.32)}$$

Table 3.4 Powder flowability and cohesiveness based on Carr Index (CI) and Hausner ratio (HR)

Classification of powder flowability based on Carr index (CI)		Classification of powder cohesiveness based on Hausner ratio (HR)	
CI (%)	**Flowability**	**HR**	**Cohesiveness**
<15	Very good	<1.2	Low
15–20	Good	1.2–1.4	Intermediate
20–35	Fair	>1.4	High
35–45	Bad		
>45	Very bad		

3.6.5 Mineral analysis

The mineral analysis was performed by scanning electron microscope (JSM-6390 LV, Japan) attached with X-ray detector to perform Energy Dispersive X-Ray Spectroscopy (EDS) [21]. As the electron beam from the SEM itself strikes the specimen surface, the electrons within the atoms of this area of interest are elevated to an excited state. When the electrons in these atoms then return to their ground state, a characteristic X-ray is emitted which yield elemental identification.

3.6.6 Amino acid compositional analysis of weaning formula

For amino acid composition analysis, the previously described protocol was followed [13, 25]. Briefly, the 500 µg protein of the optimized weaning formula was hydrolyzed with 6 N HCl at 110 ºC for 24 h under vacuum and the hydrolyzate (25 µl) was mixed with 25 µl of ortho-pthaldialdehyde (Sigma), 3-merceptopropionic acid and 9-fluorenylmethyl chloroformate (Sigma) reagents in borate buffer. This was followed by an addition of 8 µl of 1 M acetic acid and the contents were mixed thoroughly. Then, 3 µl of the resulting mixture was injected in AcclaimTM RSLC 120 C18 RP-UPLC column (2.1 mm x 100 mm, 2.2 µm particle size, 120 Å pore size) coupled to ultimate 3000RSLC (Dionex, Dreieich, Germany) UHPLC NaN_3), the amino acid derivatives were separated by eluent B (CH_3CN/MeOH/H20 in 45:45:10) at a flow rate of 0.722 ml/min. The elution was monitored initially at 338 nm for 0 -7.2 min and then at 262 nm for the next 7.2-10.5 min. The elution was monitored initially at 338 nm for 0 -7.2 min and then at 262 nm for the next 7.2-10.5 min (Gogoi, et al., 2018) (Majumdar, et al., 2014). The concentration of individual amino acid of the major protein was determined against a calibration curve of standard amino acid derivatives run in the same RP-UHPLC column under identical conditions.

3.6.7 Cytotoxicity of the developed weaning formula

XTT assay is a colorimetric assay for the nonradioactive quantification of cellular proliferation, viability, and cytotoxicity. To estimate the number of viable cells 2, 3-Bis-(2-methoxy-4-nitro5-sulfophenyl)-2H-tetrazolium-5-carboxanilide salt (XTT) is employed [6]. The mitochondria of the living cells are only capable of reducing XTT, a yellow tetrazolium salt to orange coloured formazan dye, that can be measured by absorbance at 490 (or 450) nm in a microplate reader. The major advantages of XTT assay are its sensitivity and rapid analysis since it requires no solubilization step as in MTT assay.

3.6.7.1 Cell culture

The cell line employed for this study was acute monocytic leukemia cell line (THP-1) and these cells were cultured in RPMI-1640 (Roswell Park Memorial Institute), supplemented with 10% FBS & 1% v/v penicillin/streptomycin as suggested by Hatahet et al. [16]. The seeding density of the cells was 0.3 × 106 cells/mL in canted neck flask with vent cap and further incubated in a humidified CO_2 incubator (Hamburg, Germany) with 5% CO_2 at 37°C. The cell replication was performed twice a week when the cells attended confluence.

3.6.7.2 Cellular toxicity

The cellular toxicity study was performed in acute monocytic leukemia cell line (THP-1) that were seeded at a cellular density of 300,000 cells/ml in flat bottom 24 well plate [16]. The control cells were treated with buffer and were considered 100% viable cells. The cellular viability was analyzed using 2, 3-Bis-(2-methoxy-4-nitro-5-sulfophenyl)-2H-tetrazolium-5-carboxanilide salt (XTT) assay. This assay was performed by adding 50 µl of XTT reagent to each well for 3 hours, and then absorbance was measured at 450 and 750 nm using microplate spectrophotometer (Model: Spectra Max Plus 384, Make: Molecular Devices, California, USA).

3.6.7.3 Trypan blue exclusion assay

The trypan blue exclusion assay is mainly employed to determine the number of viable cells that are present in the cell suspension. The assay is based on the principle that live cell with intact cell membranes excludes certain dyes such as trypan blue, eosin or propidium, whereas dead cells take up the dyes because of the loss of membrane selectivity. Thus, when a cell suspension is mixed with the dye and visually investigated under an optical microscope, it is observed that the viable cell is not stained whereas the nonviable cells are stained blue [11].

3.6.7.4 Cell culture

The assay was performed by the method described by Bregoli et al. [8]. The cell line employed for this study was acute monocytic leukemia cell line (THP-1) and these cells were cultured in RPMI-1640 (Roswell Park Memorial Institute), supplemented with 10% FBS & 1% v/v penicillin/streptomycin. The seeding density of the cells was 0.3 × 106 cells/mL in canted neck flask with vent cap and further incubated in a humidified incubator (Hamburg, Germany) with 5% CO_2 at 37°C. The cell replication was performed twice a week when the cells attended confluence.

3.7 In vitro starch digestibility and rheological behaviour of weaning formulation in simulated human digestive system

The digestive system or the gastrointestinal consists of the mouth, oesophagus, stomach, small and large intestines, along with glands like the salivary glands, liver, pancreas, the digestive juices with enzymes [29]. The stomach capacity of the infants is very limited and therefore proper digestion of food is very essential. Moreover, the viscosity of the food may affect the safe transport from the mouth to the stomach and therefore study of the rheological property of weaning formula is essential. The particle size of the weaning food also influences the rheological behaviour since particle size distribution of infant formula solids is subjected to transformation due to enzymatic breakdown [29]. Therefore, in this study, the in vitro digestibility and rheological behaviour of the weaning formulation with two different particle sizes i.e. 75 and 105 μm were analyzed.

3.7.1 Preparation of artificial saliva

Artificial saliva was formulated as described by Hong et al. [17]. To prepare this, $NaHCO_3$ (5.208 g), K_2HPO_4,$3H_2O$ (1.369 g), NaCl (0.877 g), KCl (0.477 g), and $CaCl_2$,$2H_2O$ (0.411 g) was separately dissolved in 100 mL of ultrapure water to make 10-fold concentrated stock solutions. Both 0.216 g of mucin (from porcine pancreas, Sigma, St. Louis, MO) and 20 000 units of α-amylase (from Aspergillus oryzae, Sigma) in combination was dispersed in 40 mL of ultrapure water. Ten milliliters of each salt stock solution was added to the protein dispersion and the total volume of artificial saliva was brought to 100 mL with distilled water. The pH of the artificial saliva was adjusted to pH 6.5, 7.0, or 7.5 with dropwise addition of 6 N HCl solution. Artificial saliva was used within 1 h of the formulation.

3.7.2 Preparation of simulated gastric fluid and intestinal fluid

Simulated gastric fluid (SGF) and simulated intestinal fluid (SIF) was prepared by the method given by Gallier et al., [12] with some modifications. SGF was prepared by dissolving 2.0 g/L of NaCl and 3.2 g of purified pepsin (800 to 2500 U/mg of protein) in 7.0 ml of HCl/L and water up to 1000 ml. the test solution had a pH of 1.2.

The simulated intestinal fluid (SIF) was prepared by mixing 6.8 g of monobasic potassium phosphate in 250 ml of water and then adding 77 ml of 0.2 N NaOH and 500 ml of water. Thereafter, 10 g of pancreatin was added and the resulting solution was adjusted with 0.2 N NaOH or 0.2 N HCl to a PH of 6.8 ± 0.1 and diluted to 1000 ml.

3.7.3 In-vitro digestibility in the simulated digestive system

The digestion procedure adapted in artificial saliva and simulated gastric and intestinal fluid will be according to the method given by Prakash [29] with some modifications.

The weaning formulations were reconstituted based on the experiments conducted to standardize the solid water ratio (article 3.5). Approximately 2 g of weaning formulation was reconstituted in 2 ml of lukewarm water. 0.1 g of artificial saliva was added to the reconstituted sample and incubated at 37°C for 10 s. thereafter, 0.5 ml of SGF was added which was incubated at 37°C for 1 h in a shaking water bath. After 1 h the sample mixture was added with 1 ml of SIF and incubated in water bath at 37°C for 2 h with gentle stirring. The first aliquots of digesta (1 ml) were removed immediately after treatment with artificial saliva and thereafter samples were drawn at an interval of 30 min for starch digestibility. The control samples included distilled water instead of enzymes. The aliquots of digesta were added to 4 ml of absolute ethanol in 10 ml tubes and immediately mixed thoroughly to stop the reaction and stored for further analysis.

3.7.3.1 Resistant starch and total starch content

The residual starch of the digested samples was estimated by measuring the glucose liberated during digestion. The glucose concentration in the digesta was measured using dinitro-salicyclic acid (DNSA) method and multiplying the absorbance by 0.9 [36].

Total starch (TS) content was determined after the dispersion of the weaning formulation in 2 M KOH (50 mg sample, 6 ml KOH) at room temperature for 30 min with constant shaking. Thereafter, hydrolysis of the solubilized sample was treated with 80 µl (1 mg/ ml) amyloglucosidase at 60°C for 45 min [14]. Glucose content was determined by using the standard dinitrosalicylic acid (DNSA) method. Total starch was calculated as glucose X 0.9.

3.7.3.2 In vitro starch digestibility

The in vitro digestibility of starch was estimated on the basis of total starch content (TS) and resistant starch (RS) determined after digestion in vitro [36] as shown below:

$$SD\ (\%) = 100\% - \left(\frac{RS}{TS}\ 100\%\right) \quad \text{Eq. (3.33)}$$

Where *SD* is the in vitro digestibility of starch, *TS* is the total starch content and *RS* is the resistant starch content

3.7.4 Rheological measurement and modeling of weaning food in the simulated digestive system

The rheological properties of the weaning formula with a different particle size (75 and 105 μm) was characterized at 37 °C using stress-controlled rheometer (Anton par, MCR 72) fitted with a parallel plate (40 mm and a gap of 1 mm). The viscosity of the infant formula samples was determined by the continuous-ramp shear rate in the range of 0.1–200·1/s as described by Prakash [29] with certain modifications. Digestion process was carried out as mentioned in section 3.7.3. After every 30 min, digestion sample was collected from the digestion bath and the viscosity was measured at a shear rate of 50·1/s. The shear rate in the digestive tract is assumed to be within this range, although there will be variability of shear rate in the mouth, stomach and intestine during the movement of food. However, for the consistency of the measurement and relative comparison, a single shear rate (50·1/s) was chosen.

3.8 Storage behaviour of weaning formula

The storage behaviour of the developed weaning formula was studied in objective #3. The detail work plan of this objective is presented in Fig. 3.4

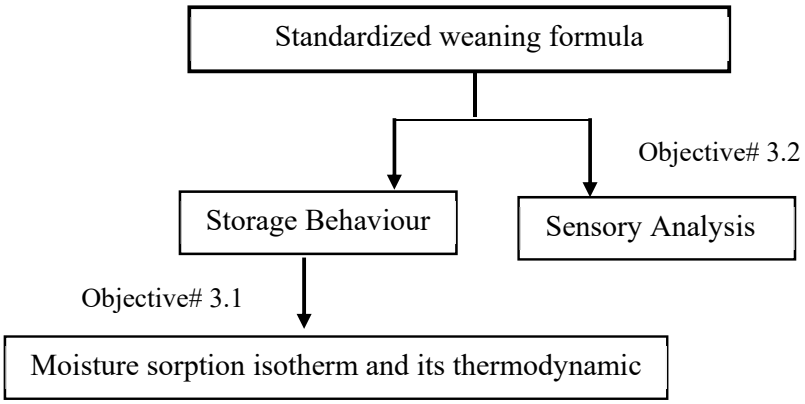

Fig. 3.4 Workplan flowchart of objective # 3

3.8.1 Moisture sorption isotherm and its thermodynamic properties

3.8.1.1 Determination of sorption isotherm

The equilibrium moisture content of the weaning formulation was estimated by the gravimetric method at four different relative humidity (45 to 90%) and at three temperatures between 20 to 40°C as described by Goula et al. [15]. The specific relative humidity in the desiccators was maintained by utilizing sulphuric acid solutions which are shown in Table 3.5.

Table 3.5 Percentage solution of H_2SO_4 used for maintaining the %ERH

% solution of H_2SO_4	% ERH		
	20°C	30°C	40°C
45	0.45	0.46	0.47
40	0.55	0.57	0.58
35	0.66	0.66	0.67
30	0.74	0.75	0.76
15	0.92	0.92	0.92

The weaning formulation was weighed (3 ± 0.01g) and placed in weighed aluminum dishes which were dried at 45°C in an air-circulated oven over silica gel for 3 days to remove any moisture. Thereafter, the samples were kept in desiccators over sulphuric acid solutions of known relative humidity. These desiccators were placed in temperature-controlled cabinets maintained at temperatures 20, 30 and 40°C (± 1°C) and the equilibrium condition was determined when the weight change in successive reading was less than ± 0.001g. This involved a period of 30 days approximately. The time used for removal, weighing, and putting back the sample in the desiccator was about 30 s which reduced the degree of atmospheric moisture sorption during weighing. The equilibrium moisture content was determined by vacuum method at 70°C until constant weight. All the measurements were analyzed in triplicates.

3.8.1.2 Modelling of sorption isotherm

The plots of equilibrium moisture content of weaning formula and the corresponding water activity at three temperatures were used to generate sorption isotherms. The weaning formula was dried to the lowest water activity (i.e. a_w=0.08) before exposing for sorption study and therefore all the curves generated were adsorption isotherms. Five different sorption models (Eq 3.34-3.38) were selected for the fitting of sorption data [15].

GAB Model $$M_e = \frac{M_0 C K a_w}{(1 - K a_w)(1 - K a_w + C K a_w)}$$ Eq. 3.34

Peleg Model $$M_e = k_1 a_w^{n_1} + k_2 a_w^{n_2}$$ Eq. 3.35

Henderson Model $$M_e = \left[\frac{ln(1 - a_w)}{-A}\right]^{1/B}$$ Eq. 3.36

Smith Model $$M_e = A + B ln(1 - a_w)$$ Eq. 3.37

Oswin Model $$M_e = A \left[\frac{a_w}{1 - a_w}\right]^B$$ Eq. 3.38

Where M_e is the equilibrium moisture content (kg/kg dry solid); aw is water activity or relative humidity; *A* and *B* are constants; M_0 is the monolayer moisture content; *C* and *K* are constants related to the energies of interaction between the first and further molecules at the individual sorption sites; k_1 and k_2 are model parameters.

A non-linear least-square regression analysis was done to evaluate the models. The curve fitting and regression analysis were performed using curve fitting tool of MATLAB. The goodness of fit for the models was evaluated with the sum of square error due to fit (*SSE*), the percent root means square error (*RMSE*) and adjusted correlation coefficient (R^2) values. The equation giving the smallest *SSE, RMSE* and highest adjusted R^2 values was considered to be best fitted. The measures of error in terms of *SSE*, *RMSE* and R^2 are calculated using the following equations:

$$SSE = \Sigma_{i=1}^{n} w_i \left(M_i - \widehat{M_i}\right)^2$$ Eq. 3.39

$$RMSE = \sqrt{\frac{SSE}{n-m}}$$ Eq. 3.40

Where, M_i is the experimental EMC, $\widehat{M_i}$ is the predicted EMC from the fitting curve, w_i is the weighting applied to each data point and was set to unity in this analysis. Here, *n* is the number of experimental data point and *m* is the number of coefficients in each equation.

3.8.1.3 Thermodynamic properties of sorption phenomenon

The net isosteric heat ($q_{st,n}$) is defined as the total heat of sorption in the food minus the heat of vaporization of water, at the system temperature [1] and this is determined by the Clausius-Clayperon equation as shown below:

$$\left[\frac{d(lna_w)}{d\left(\frac{1}{T}\right)}\right]_M = \frac{Q_{st,n}}{R} \quad \text{Eq. 3.41}$$

$$Q_{st,n} = Q_{st} - \Delta H_{vap} \quad \text{Eq. 3.42}$$

Where a_w is the water activity, T is temperature (K), $Q_{st,n}$ is the net isosteric heat of sorption (kJ/mol water), Q_{st} is the isosteric heat of sorption (kJ/mol water), ΔH_{vap} is heat of vaporization of water in pure form (kJ/mol water), R is the universal gas constant (8.314J/mol K)

The graph of the natural logarithm of the water activity (a_w) was plotted against the inverse of absolute temperature. The net isosteric heat of sorption was calculated from the slope of the regression line. The sorption entropy (ΔS) is related to the net isosteric heat of sorption and it denotes the energy associated with the sorption sites. It can be derived from Eq 3.43 which is given below

$$-ln(a_w) = \frac{Q_{st,n}}{RT} - \frac{\Delta S}{R} \quad \text{Eq. 3.43}$$

The predicted coefficients of Peleg model (best-fitted model) and GAB model suggested for most biological material [1] were used to determine the sorption entropy at specific moisture content. It was calculated from the intercept (ΔS/R) of the fitted curve of ln (a_w) versus 1/T.

This approach assumes that qst is invariant with temperature, with the application of the method requiring measurement of sorption isotherms at more than two temperatures.

An empirical exponential relationship between the isosteric heat of sorption and the moisture content was used as described by Goula et al. [15].

$$q_{st} = q_0 \exp(-\frac{X}{X_0}) \quad \text{Eq. 3.44}$$

where q_0 is the isosteric heat of sorption of the first molecule of water in the food in kJ/mol, and X_0 is a characteristic moisture content of the food material in kg/kg dry solid, at which this isosteric heat of sorption has been reduced by 63%. The constants q_0 and X_0 are estimated by fitting Eq. 3.44 to the values of q_{st}, obtained by applying Eq. 3.41 to experimental isotherms.

A plot of Q_{st} versus ΔS from values of Eq. (3.43) can be obtained for each set of sorption data and thereafter, these values can be correlated according to the following equation:

$$\Delta H = T_B \Delta S + \Delta G_B \quad \text{Eq. 3.45}$$

where T_B is the isokinetic temperature, representing the temperature at which all reactions in the sorption series proceed at the same rate. A high degree of linear correlation between enthalpy and entropy can be observed and thus the compensation theory can be accepted to be valid for sorption. The isokinetic temperature can be compared with the harmonic mean temperature, T_{hm}, which is defined as

$$T_{hm} = \frac{n}{\sum_{i=1}^{n}(1/T)} \quad \text{Eq. 3.46}$$

where n is the number of isotherms.

According to literature, a linear chemical compensation pattern exists only if $T_B \neq T_{hm}$. If $T_B > T_{hm}$ the process is enthalpy driven, while if the opposite condition is observed, the process is considered to be entropy-controlled [15].

The Gibb's free energy indicated the sorbent's affinity for water and refers to the weather or not the sorption is a spontaneous process [41]. It was calculated for the weaning formulation as given below

$$\Delta G = -R\,T\,\ln(a_w) \quad \text{Eq. 3.47}$$

Water activity data generated from Paleg and GAB model at specific equilibrium moisture content were used to calculate Gibb's free energy change at different absolute temperatures.

3.8.2 Determination of quality changes in weaning formula

The quality parameters of weaning formula were determined at 40°C by taking one pouch at a time from desiccator at an interval of 10 days. The free fatty acid (FFA) was estimated by the titration method. The acid value of oil is defined as the number of milligrams of potassium hydroxide required to neutralize the free fatty acids present in one gram of fat. The FFA of weaning formula was measured by directly titrating the oil/fat in an alcoholic medium against standard potassium hydroxide/sodium hydroxide solution. Another parameter peroxide value (PV) was also estimated. Peroxide value is mainly the measurement of the peroxides contained in the sample. It was determined by titrating the sample against thiosulphate in the presence of potassium iodide (KI) and starch was used as an indicator [31].

3.9 Sensory evaluation

The weaning formula was reconstituted with water and subjected to sensory evaluation to test their acceptability using a nine-point hedonic scale (1 for dislike extremely and 9 for like extremely) in terms of taste, aroma, consistency, mouthfeel and overall acceptability when compared to commercialized product. A total of 30 trained and semi-trained panelist was involved in the sensory evaluation from the Department of Food Engineering and Technology, Tezpur University.

3.10 Statistical Analysis

3.10.1 Chemometric analysis

Chemometrics mainly involves use of mathematical and statistical methods to improve the understanding of chemical information and to correlate quality parameters or physical properties to analytical instrument data. In this study two chemometric technique viz. principle component analysis (PCA) and partial least squares (PLS) were performed [23, 38] to inter-relate independent variables (time of malting and data on the spectra emission intensities at different wavelengths) and dependent variables (contents of amylose, amylopectin, total starch and reducing sugars). The spectrum was obtained from Raman spectrophotometer and FTIR. The data were pre-processed using the FFT algorithm where 5-points were used to minimize the problems due to baseline shift of different starch samples. The data of the spectra emission intensities at different wavelength were considered as the independent variables whereas the parameters that depict the changes during malting process viz. amylose, amylopectin, total starch and reducing sugar contents were considered as dependent variables. The algorithm employed was NIPALS and the optimal number of components were analyzed by the method of cross-validation. The v-fold cross-validation was used where the data was divided into v-segments which were used to build the model and the remaining was used for testing. The process was then repeated for all possible permutations of the training and testing segments. The performance of the models was evaluated by the root mean square error of prediction (RMSEP).

Analysis of variance (ANOVA) in this study was performed using IBM Statistical Package for the Social Sciences (SPSS, version 20). Duncan's multiple range test (DMRT) was performed to identify the terms having significant differences at $p \leq 0.05$. Pearson correlation analysis was also conducted to determine the relationships between/among the pasting and thermal properties.

Bibliography

[1] AL-Muhtaseb, A. H., McMinn, W. A. M., and Magee, T. R. A. Moisture sorption isotherm characteristics of food products: a review. *Trans IChemE,* 80:118-127, 2002.

[2] Asante, E., Adjaottor, A. A., and Woode, M. Y. Malting characteristics of Wita 7 variety of rice. *Peak Journal of Food Science and Technology,* 1: 61-67, 2013.

[3] Association of Official Analytical Chemists. *Official Methods of Analysis*, Washington D.C, 1990.

[4] Ayernor, G. S., and Ocloo, F. C. K. Physico-chemical changes and diastatic activity associated with germinating paddy rice (PSB.Rc 34). *African Journal of Food Science,* 1:037–041, 2007.

[5] Bas, D., Dudak, F. C., and Boyacı, I. H. Modeling and optimization III: Reaction rate estimation using artificial neural network (ANN) without a kinetic model. *Journal of Food Engineering,* 79:622–628, 2007.

[6] Berridge, M. V., Herst, P. M., and Tan, A. S. Tetrazolium dyes as tools in cell biology: New insights into their cellular reduction. *Biotechnology Annual Review,* 11:127-152, 2005.

[7] Bhadra, A., Bandyopadhyay, A., Chakraborty, S., Roy, S., and Kumar, T. Development and Testing of an ANN Model for Estimation of Runoff from a Snow-Covered Catchment. *Journal of the Institution of Engineers (India): Series A,* 98:29-39, 2017.

[8] Bregoli, L., Chiarinia, F., Gambarelli, A., Sighinolfi, G., Gatti, A. M., Santia, P., Martelli, A. M., and Coccoa, L. Toxicity of antimony trioxide nanoparticles on human hematopoietic progenitor cells and comparison to cell lines. *Toxicology,* 262:121–129, 2009.

[9] Chakraborty, S., Sarma, M., Bora, J., Faisal, S., and Hazarika, M. K. Generalization of drying kinetics during thin layer drying of paddy. *Agricultural Engineering International: CIGR Journal,* 18:177-189, 2016.

[10] Cornejo, F., and Rosell, C. M. Influence of germination time of brown rice in relation to flour and gluten free bread quality. *Journal of food science and technology,* 52: 6591–6598, 2015.

[11] Freitas, B. A. A., Almeida, V. G., Pinto, M. C. X., Mourao, F. A. G., Massensini, A. R., Filho, O. A. M., Vieira, E. R., and Melo, G. E. A. B. Trypan blue exclusion assay by flow cytometry. *Brazilian Journal of Medical and Biological Research,* 47:307-315, 2014.

[12] Gallier, S., Ye, A., and Singh, H. Structural changes of bovine milk fat globules during in vitro digestion. *Journal of dairy science,* 95:3579-3592, 2012.

[13] Gogoi, D., Arora, N., Kalita, B., Sarma, R., Islam, T., Ghosh, S. S., Devi, R., and Muherjee, A. K. Anticoagulant mechanism, pharmacological activity, and assessment of preclinical safety of a novel fibrin (ogen) olytic serine protease from leaves of Leucas indica. *Scientific reports,* 8:6210, 2018.

[14] Goni, I., Garcia-Alonso, A., and Saura-Calixto, F. A starch hydrolysis procedurecto estimate glycemic index. *Nutrition Research,* 17:427–437, 1997.

[15] Goula, A. M., Karapantsios, T. D., Achilias, D. S., and Adamopoulos, K. G. Water sorption isotherms and glass transition temperature of spray dried tomato pulp. *Journal of Food Engineering,* 85:73–83, 2000.

[16] Hatahet, T., Morille, M., Shamseddin, A., Aubert-Pouessel, A., Devoisselle, J. M., and Bégu, S. Dermal quercetin lipid nanocapsules: Influence of the formulation on antioxidant activity and cellular protection against hydrogen peroxide. *International journal of pharmaceutics,* 518:167-176, 2017.

[17] Hong, Y.-H., Park, J.-Y., Park, J.-H., Chung, M.-S., Kwon, K.-S., Chung, K., Won, M., and Song, K.-B. Inactivation of Enterobacter sakazakii, Bacillus cereus, and Salmonella typhimurium in powdered weaning food by electron-beam irradiation. *Radiation Physics and Chemistry,* 77:1097– 1100, 2008.

[18] Jinapong, N., Suphantharika, M., and Jamnong, P. Production of instant soymilk powders by ultrafiltration, spray drying and fluidized bed agglomeration. *Journal of Food Engineering,* 84:194-205, 2008.

[19] Kapoor, R., and Metzger, L. E. Small-scale manufacture of process cheese using a rapid visco analyzer. *Journal of Dairy Science,* 88:3382–3391, 2005.

[20] Kizil, R., Irudayaraj, J., and Seetharaman, K. Characterization of Irradiated Starches by Using FT-Raman and FTIR Spectroscopy. *Journal of Agricultural and Food Chemistry,* 50:3912-3918, 2002.

[21] Konishi, Y., Hirano, S., Tsuboi, H., and Wada, W. Distribution of Minerals in Quinoa (Chenopodium quinoa Willd.) Seeds. *Bioscience, Biotechnology, and Biochemistry,* 68:231-234, 2004.

[22] Labuschagne, M., Phalafala, L., Osthoff, G., and Biljon, A. V. The influence of storage conditions on starch and amylose content of South African quality protein maize and normal maize hybrids. *Journal of Stored Products Research,* 56:16-20, 2014.

[23] Lawless, H. T., and Heymann, H. *Data relationships and multivariate applications. In: Sensory evaluation of food: principles and practices*. New York: Chapman and Hall, 1998.

[24] Ludikhuyze, L., Ooms, V., Weemaes, C., and Hendrickx, M. Kinetic study of the irreversible thermal and pressure inactivation of myrosinase from broccoli (*Brassica oleracea* L. cv. Italica). *Journal of Agricultural and Food Chemistry,* 47:1794-1800, 1999.

[25] Majumdar, S., Sarmah, B., Gogoi, D., Banerjee, S., Ghosh, S. S., Banerjee, S., Chattopadhyay, P., and Mukherjee, A. K. Characterization, mechanism of anticoagulant action, and assessment of therapeutic potential of a fibrinolytic serine protease (Brevithrombolase) purified from *Brevibacillus brevis* strain FF02B. *Biochimie,* 103:50-60, 2014.

[26] Mir, S. A., and Bosco, S. J. D. Cultivar difference in physicochemical properties of starches and flours from temperate rice of Indian Himalayas. *Food Chemistry*, 157:448–456, 2014.

[27] Olugbile, A., Obadina, A. O., Atanda, A. O., Omemu, O. B., and Olatope, S. O. A. Physicochemical Changes and Diastatic Activity Associated with Germination of 'Boromo', a Paddy Rice Variety from Western Nigeria. *Journal of Food Processing and Preservation,* 39:116-122, 2015.

[28] Park, I.-M., Ibanez, A. M., Zhong, F., and Shoemaker, C. F. Gelatinization and Pasting Properties of Waxy and Non-waxy Rice Starches. *Starch,* 59:388–396, 2007.

[29] Prakash, S., Ma, Q., and Bhandari, B. Rheological behaviour of selected commercially available baby formulas in simulated human digestive system. *Food research international,* 64:889-895, 2014.

[30] Quadir, N., Wani, S. A., Bhat, B. A., Wani, T. A., and Quraazah, A. Germination behavior of some Kashmiri paddy cultivars. *Journal of Chemical, Biological and Physical Sciences, 2*:1820–1829, 2012.

[31] Sadasivam, S., and Manickam, A. *Biochemical methods.* New Delhi: New Age International Limited, 2005.

[32] Sajilata, G., Singhal, R. S., and Kulkarni, P. R. Weaning foods: A review of the Indian experience. *Food and Nutrition Bulletin,* 23:208-226, 2002.

[33] Saqib, A. A. N., and Whitney, P. J. Differential behaviour of the dinitrosalicylic acid (DNS) reagent towards mono- and di-saccharide sugars. *Biomass and Bioenergy,* 35:4748–4750, 2011.

[34] Sawant, A. A., Thakor, N. J., Swami, S. B., and Divate, A. D. Physical and sensory characteristics of Ready-To-Eat food prepared from finger millet based composite mixer by extrusion. *Agricultural Engineering International: CIGR Journal,* 15:100-105, 2013.

[35] Sun, Q., Gong, M., Li, Y., and Xiong, L. Effect of dry heat treatment on the physicochemical properties and structure of proso millet flour and starch. *Carbohydrate Polymers,* 110:128–134, 2014.

[36] Swieca, M., Baraniak, B., and Gawlik-Dziki, U. In vitro digestibility and starch content predicted glycemic index and potential in vitro antidiabetic effect of lentil sprouts obtained by different germination techniques. *Food Chemistry,* 138:1414–1420, 2013.

[37] Tian, B., Xie, B., Shi, J., Wu, J., Cai, Y., Xu, T., Xue, S., and Deng, Q. Physicochemical changes of oat seeds during germination. *Food Chemistry,* 119:1195–1200, 2010.

[38] Tiwari, S., Ravi, R., and Bhattacharya, S. Dehumidifier assisted drying of a model fruit pulp-based gel and sensory attributes. *Journal of Food Science,* 77:263–273, 2012.

[39] Wu, F., Chen, H., Yang, N., Wang, J., Duan, X., Jin, Z., and Xu, X. Effect of germination time on physicochemical properties of brown rice flour and starch from different rice cultivars. *Journal of Cereal Science,* 58:263-271, 2013.

[40] Yin, H., Chen, Z., Gu, Z., and Han, Y. Optimization of natural fermentative medium for selenium-enriched yeast by D-optimal mixture design. *LWT - Food Science and Technology,* 42:327–331, 2009.

[41] Yogendrarajah, P., Samapundo, S., Devlieghere, F., De Saeger, S., and De Meulenaer, B. Moisture sorption isotherms and thermodynamic properties of whole black peppercorns (Piper nigrum L.). *LWT - Food Science and Technology,* 64:177-188, 2015.